Materials Innovation toward Establishment of the Advanced Waste-to-Energy Recovery System

Masayuki Yoshiba
Graduate School of Engineering, Tokyo Metropolitan University
Hachioji, Tokyo 192-0397, Japan
Fax: 81-426-77-2717, e-mail: yoshiba@ecomp.metro-u.ac.jp

In order to evaluate an applicability of the existing corrosion-resistant alloys as the boiler superheater of an advanced high-efficiency municipal solid waste-to-power generation plant of which environment is characterized by the much severe high-temperature corrosion, the corrosive failure analyses were conducted for twenty kinds of the mainly commercial alloys from different aspects. Corrosive failure in such an aggressive environment was revealed to be characterized by the localized attack-dominating mode, namely along the grain boundary, for almost all systems of the alloys. On the basis of the failure analyses, a guideline for the high-performance alloy design to withstand against the high-temperature corrosive environment was discussed to make a proposal from both the compositional and microstructural viewpoints.

Key words: Municipal Solid Waste (MSW) Incineration Plant, Waste-to-Power Generation, High-Temperature Corrosion, Intergranular Corrosion, Chlorination, Corrosion-Resistant Alloys

1. INTRODUCTION

Waste-to-power generation is one of the most promising energy recovery means both in the municipal solid waste (MSW) incineration plant, and in near future in the combined type of thermal decomposition and gasification of waste together with ash melting system by which high quality of the materials recycling also is possible. In order to improve an efficiency of the waste-to-power generation, it is required for the superheated steam temperature to be much increased by the MSW boiler up to around 500 ℃ . This means for the hot section components such as superheater tube to be subject to very severe and complicated corrosion attack which can be caused by both the aggressive molten salt containing multicomponents of chloride eutectics and the corrosive flue gases rich in chlorides.

There is several approaches to mitigate the high-temperature corrosion problem; (1) modification of the furnace and boiler design to minimize an ash deposition onto the alloy-tube surface, (2) environmental control to minimize the corrosivity and (3) materials innovation to overcome the corrosive damage. In order to establish more sophisticated waste-to-power plant, then, these different technological aspects must be evolved with a harmonization, since the corrosive environment is too severe at present to be soluble solely by anykind technical approach described above [1].

In the present study, a guideline for the alloy design to withstand against the high-temperature aggressive environment of the high-efficiency waste-to-power plant will be discussed to make a proposal from the materials viewpoint on the basis of the systematic corrosion failure analysis for different kinds of the corrosion-resistant alloys.

2. MATERIALS AND EXPERIMENTAL

Twenty kinds of the mainly commercial alloys were adopted in the high-temperature corrosion test, containing carbon and low-alloy steels, stainless steels, Ni-base and Co-base alloys, together with pure Ni and Cr. These alloys chemistry is listed in Table Ⅰ . These alloys were heat-treated according to the specification for each alloy. Then, the specimens for corrosion test were machined to the rectangular shape with dimensions 10 x 10 with (1 ～ 4) mm thickness, followed by the emery polishing through 500 grit and degreasing by acetone.

High-temperature corrosion testing was conducted by means of the ash coating method according to the JSPS methodology [2]. Then, the ash precoated was collected from four cities of MSW incineration plants in Japan and blended evenly, of which chemical composition is listed in Table Ⅱ . The quantity of ash precoated was 40 mg/cm ^{2} onto the entire specimen surface. The specimens precoated were settled in the apparatus which was then inserted into the flue gas path of an actual MSW incineration plant in Tokyo, as schematically shown in Fig. 1. This manner of corrosion testing should have an advantage in providing more controlled corrosive environment by using a given amount of ash precoated and supplying an actual flue gas bypassed, as compared with the conventional laboratory corrosion tests under the much simplified condition. This manner of testing will be termed as the actual furnace gas test. Flue gas temperature measured was 660 ℃ in average, which should be denoted as the nominal test temperature, although it was fluctuated in the range between 600 and 680 ℃ during the testing period. This temperature condition should be considered as one of the extreme, since the target metal temperature in near future is still

Table I Chemical composition of various commercial alloys adopted (mass%).

Alloys	C	Si	Mn	P	S	Ni	Cr	Mo	Fe	Co	W	Nb +Ta	Others
STB 35	0.11	0.19	0.45	0.010	0.001				Bal.				
STB A24	0.12	0.26	0.42	0.014	0.006		2.13	0.94	Bal.				
STB A27	0.06	0.29	0.49	0.016	0.001		9.09	2.05	Bal.				
SUS 405	0.05	0.45	0.44	0.021	0.003	0.18	13.38		Bal.				Al 0.19
SUS 430	0.05	0.47	0.39	0.032	0.018	0.15	16.31		Bal.				
SUS 304	0.05	0.39	1.35	0.030	0.003	8.10	18.18		Bal.				
SUS 309S	0.08	0.27	1.62	0.027	0.001	13.10	22.22		Bal.				
SUS 310S	0.02	0.35	1.14	0.021	<0.001	19.35	24.55		Bal.				
SUS 316	0.05	0.31	1.12	0.039	0.023	10.09	16.05	2.05	Bal.				
SUS XM15J1	0.06	3.71	0.41	0.029	0.003	13.04	18.51		Bal.				Cu 0.68
HK 40	0.40	0.70	0.65	0.019	0.011	22.01	25.18	0.08	Bal.				
Incoloy 800H	0.09	0.02	0.09		0.003	31.6	20.4		Bal.				Al 0.40 Ti 0.30
Pure Ni	0.003	0.10	0.11		0.001	Bal.			0.06				Cu 0.01
Inconel 601	0.03	0.13	0.26		<0.001	Bal.	22.57		13.84				Cu 0.22 Al 1.31
Inconel 625	0.035	0.11	0.33	0.005	<0.001	Bal.	21.72	8.82	3.36	0.27		3.75	Al 0.17 Ti 0.32
Hastelloy X	0.07	0.27	0.51	0.013	<0.001	Bal.	21.15	8.53	18.57	1.51	0.52		Cu 0.23
50Ni−50Cr	0.013	0.66	0.19	0.001	0.002	Bal.	47.80					1.47	
HA 188	0.099	0.36	0.75	0.006	0.001	22.75	22.19	0.25	1.49	Bal.	14.02		Cu 0.010
Stellite 6	1.33	1.25	0.02			2.60	28.6	0.20	2.75	Bal.	4.90		
Pure Cr	0.01	0.01					99.7	0.02	0.25		0.03		

Table II Chemical composition of the ash mixture collected from four cities of the MSW plants (mass%).

Al	Si	Fe	Na	K	Ca	Mg	Pb	Zn	T−S	T−Cl	H_2O
3.80	5.07	1.72	6.43	7.77	14.20	1.56	0.78	1.95	13.45	2.06	0.43

Table III Analytical data of the flue gas composition (partly by the value converted).

O_2 (%)	NO_X (ppm)	SO_X (ppm)	HCl (ppm)	CO (ppm)	CO_2 (%)	H_2O (%)
11.3 ~ 12.3	77 ~ 110	30 ~ 75	175 ~ 465	80 ~ 100	8 ~ 10	15 ~ 20

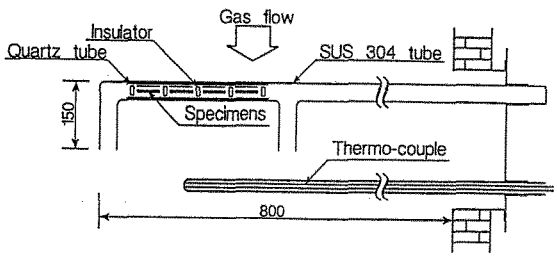

Fig. 1 Schematic view of apparatus for the actual furnace gas test.

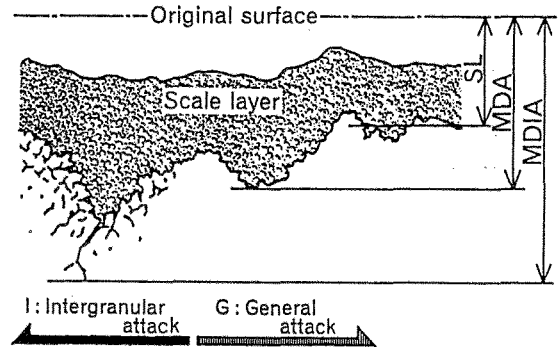

Fig. 2 Schematic illustration showing different types of corrosion morphologies and measuring methods.

put at around 550 ℃ . Typical data of the flue gas analyses are summarized in Table III . The actual furnace gas test was carried out for 96h, by using three specimens for each alloy and the same testing condition.

After the corrosion test, corrosive damage of all the specimens were evaluated mainly by means of the metallography and X-ray micro-analysis for the specimen cross-section. In particular, different measures of the depth of attack were adopted to characterize the corrosion morphology, as schematically shown in Fig. 2.

3. RESULTS AND DISCUSSION

3.1 Corrosive failure analysis

Figure 3 shows the summary for different measures of the depth of corrosive attack. Here, the average depth of attack (ADA) is a mean value for the maximun depth of attack (MDA) or the maximum depth of intergranular attack (MDIA) that is obtainable from all the specimen cross-sections examined. Then, it isindicative that the larger both MDA or MDIA and ADA extend, the more localized corrosive attack is easy to occur. It is found that almost all the systems of alloys are subject to a localized attack, namely to an intergranular attack. In particular, it should be noted that almost all stainless steels except for SUS XM15J1 are subjected to an intergranular attack, suggesting the requirement for the alloy design not to induce an intergranular attack. Consequently, the stainless steel development for such an application is focused recently in Japan on reducing the grain boundary corrosion sensitivity by modifying the C and N contents, with combination of the carbide forming additives such as Mo

and Nb, in order to prevent a development of the Cr-depleted zone along grain boundary [3]. For instance, several kinds of the modified 310 or 309 class stainless steels have been newly developed, such as 310J1 with lower C and Nb addition, 309J2 with substituting N for C and Mo addition, respectively [1].

From Fig. 3, the Cr content is found necessary of more than 20% at least to insure the improved corrosion resistance in such an aggressive environment. However, increasing in a Cr content does not always bring about an improved corrosion resistance, as can be seen for pure Cr. Pure Cr was found to be easily subject to a general corrosion probably by the oxy-chlorination reaction process, of which products; ie. CrO_2Cl_2, is highly volatile in the atmosphere in which substantial amount of chlorides such as HCl and oxygen coexist.

Among all the alloys tested, Inconel 625 exhibited the best corrosion resistance with suffering from no intergranular attack. Inconel 601 is somewhat inferior to the 625 alloy, suggesting a beneficial effect of Mo addition.

3.2 Morphological features of corrosion

From the detailed metallographic examination of all the specimen cross-sections, it was revealed that the onset or nucleation of corrosion is characterized in general by the very small magnification of corrosion-pit formation. This form of corrosion seems to be attributed to the fact that small fraction of ash deposited can be molten at the testing temperature to play locally a fluxing action against the protective oxide films such as Cr_2O_3. According to the ash analyses by using DTA-TG and XRD, a number of endothermic peak was detected to be suggestive for many kinds of the low-melting eutectics composed of mainly chlorides and/or partly sulphates rich in K, Na and containing small amount of heavy metals such as Zn and Pb to be molten even in the lower temperature regime between 180 and 512 °C [1]. Lai has summarized the melting points for many kinds of the low-melting chloride eutectics, as shown in Table Ⅳ [4]. It is apparent that almost all the low-melting chloride eutectics are associated with the alkali and/or heavy metals. Consequently, these eutectics in the ash deposits should be able to melt locally to induce a pitting corrosion in the early stage, which is subsequently followd by the propagation stage of corrosion still by the locallized attack dominating manner, as previously proposed by author on the basis of the exposure test [5].

In the corrosion propagation stage too, characteristic manners of the localized attack was observed in many alloy specimens. For 50Ni-50Cr alloy, in particular, a corrosion attack was found to occur preferentially along the secondary α ' phase which is composed dominantly of Cr, as shown in Fig. 4. This seems to be caused by the preferential oxy-chlorination reaction of α ' phase of which products are highly volatile, as in the case of pure Cr. Consequently, 50Ni-50Cr alloy exhibited rather increased value in the maximum depth of attack, in spite of the minimized surface loss as shown in Fig. 3. Thus, it should be noted for an alloy design toward a much improved corrosion resistance in such a waste-to-power plant not to develop anykind of the second phase which can induce a preferential attack.

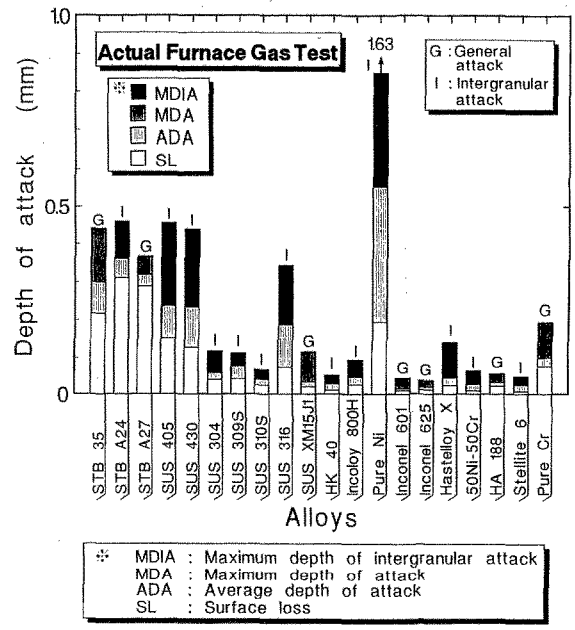

Fig. 3 Summary of different measures of the depth of attack together with the corrosion morphologies observed in the actual furnace gas test.

Table Ⅳ Melting points of different kinds of the low-melting chloride eutectics [4].

Eutectic mixture, mole%	Melting point, °C
$25NaCl-75FeCl_3$	156
$37PbCl_2-63FeCl_3$	175
$60SnCl_2-40KCl$	176
$70SnCl_2-30NaCl$	183
$70ZnCl_2-30FeCl_3$	200
$20ZnCl_2-80SnCl_2$	204
$55ZnCl_2-45KCl$	230
$70ZnCl_2-30NaCl$	262
$60KCl-40FeCl_2$	355
$58NaCl-42FeCl_2$	370
$70PbCl_2-30NaCl$	410
$52PbCl_2-48KCl$	411
$72PbCl_2-28FeCl_2$	421
$90PbCl_2-10MgCl_2$	460
$80PbCl_2-20CaCl_2$	475
$49NaCl-50CaCl_2$	500

3.3 Concept for the corrosion-resistant alloy design

On the basis of the corrosive failure analyses for various alloys in the actual furnace gas test, the improved corrosion-resistance alloy design concept can be conducted as follows. Figure 5 shows the isocorrosion contour in terms of the MDA or MDIA

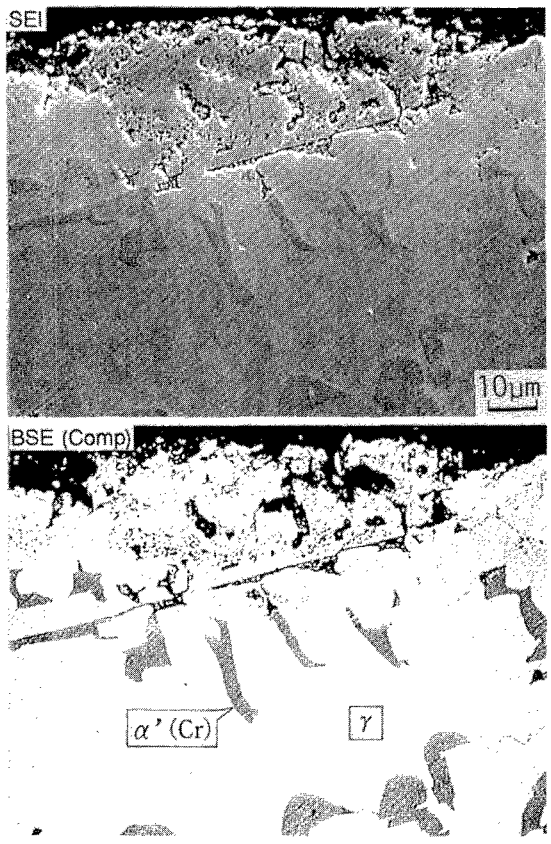

Fig. 4 Typical corrosion morphology by SE and BS image modes at the cross-sectional surface zone of 50Ni-50Cr alloy specimen.

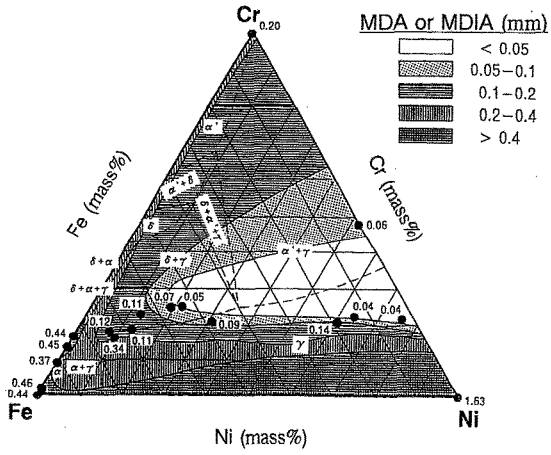

Fig. 5 Isocorrosion contours in terms of MDA or MDIA for various alloy specimens.

which can be obtained by plotting the data for various alloys in Fig. 3. Here, the 650 ℃ isothermal phase diagram for Fe-Ni-Cr ternary alloy also was superposed in convenience [6]. It should be noteworthy that for ternary Fe-Ni-Cr alloy the most promising composition is lie in the regime of the γ single phase with the alloy composition rich in Ni and Cr of more than about 30% and 20%, respectively, although the data plotted can not cover entirely the ternary compositional area.

The window for such a beneficial composition range is expected to become possible to extend widely with the temperature lowers. As regards the other alloying additives since the fourth, furthermore, it seems much effective to make an addition of appropriate amount of the backup elements such as Mo and/or Nb which can play both roles as a grain boundary stabilizer and an inhibiter against the chlorination-dominating attack toward alloy substrate during from the break down to the healing or rejuvenation of the protective oxide films such as mainly Cr_2O_3. In such a case, of course, it should be still important to make sure the phase stability of γ .

4. CONCLUDING REMARKS

Corrosive failure analysis was conducted for twenty kinds of the commercial corrosion-resistant alloys for an application of advanced high-efficiency waste-to-power plant components. Main results obtained are as follows.

(1) Almost all systems of the alloys were easily subjected to either an intergranular attack or the other mode of localized attack.

(2) The best corrosion-resistance was found for the Ni-base Inconel 625 alloy with suffereing from no localized attack.

(3) On the basis of the corrosive failure analyses, an appropriate alloy design concept to overcome against the aggressive environment was discussed to make a proposal in relation with the aspects of both the principal alloy composition and microstructure.

ACKNOWLEDGMENT

Author will wish to acknowledge the Japan Waste Research Foundation for supporting in the materials and so forth. The experimental works were carried out competently by Mr. S. Takasugi of TMU, Mr. A. Motoi and Dr. T. Urabe of Tokyo Metropolitan Government.

REFERENCES

1. M. Yoshiba, Report the 123rd Committee, Japan Soc. Promotion Sci., 38, 319-333 (1997) (in Japanese).
2. The 123rd Committee of JSPS, Report the 123rd Committee, Japan Soc. Promotion Sci., 14, 255-6 (1973) (in Japanese).
3. N. Otsuka, A. Natori, T. Kudo and T. Imoto, Corrosion/94, Paper No. 401, NACE, (1994).
4. G. Y. Lai, High-Temperature Corrosion of Enginering Alloys, ASM Int'l., (1990), p. 158.
5. M. Yoshiba, H. Notani, S. Uno and N. Hirayama, Proc. 13th Int'l. Corrosion Conf., ACA, 1384-1393 (1996).
6. P. Marshall, Austenitic Stainless Steels -Microstructure and Mechanical Properties, Elsevier Appl. Publ., (1984), p. 14.

(Received December 11, 1998; accepted March 15, 1999)